ISET Journal of Earthquake Technology, Paper No. 503, Vol. 46, No. 2, June 2009, pp. 47–64

PERFORMANCE OF EXTERIOR BEAM-COLUMN JOINTS UNDER SEISMIC TYPE LOADING

K.R. Bindhu*, P.M. Sukumar** and K.P. Jaya**

*Department of Civil Engineering
College of Engineering, Thiruvananthapuram-695016
**Structural Engineering Division
Anna University, Chennai-600025

ABSTRACT

The objective of the present study is to compare the behaviour of exterior beam-column joint sub-assemblages with transverse reinforcements detailed as per IS 456 and IS 13920. A six-storeyed RC building in the zone III is analyzed, and one of the exterior beam-column joints at an intermediate storey is designed. The earthquake analysis and design are carried out by incorporating all the modifications as per the latest revisions of IS 1893 and IS 13920. Four one-third scaled specimens, two detailed as per IS 456 and SP 34 and the other two as per IS 13920, were tested under a reverse cyclic loading. The specimens were tested under two different axial loads to evaluate the effect of axial load on the behaviour of joints. The test results indicate that the latest revisions for joint design assure the beam failure to take place before the joint failure. Enhancements in the performance of beam-column joints detailed as per IS 13920 in the reversal of loading were also observed.

KEYWORDS: Beam-Column Joint, Confinement, Detailing, Seismic Analysis, Strong-Column Weak-Beam Concept

INTRODUCTION

Severe reverse cyclic loading due to earthquakes causes large inelastic deformations in the beam-column joints of high-rise buildings. If the joints are not designed and detailed properly, their performance can significantly affect the overall response of the moment-resisting frames. Due to the restriction of space available in the joint block, the detailing of joint reinforcement assumes more significance than elsewhere. One of the basic assumptions of the frame analysis is that the joints are strong enough to sustain the forces (i.e., moments, and axial and shear forces) generated by the loading, and to transfer the forces from one structural element to another (i.e., from beams to columns in most of the cases). The analysis with the assumption of joint being rigid fails to consider the effects of high shear forces developed within the joint (Subramanian and Rao, 2003).

Recent earthquakes have demonstrated that even when the beams and columns in a reinforced concrete frame remain intact, the integrity of the whole structure is compromised if the joints, where these members are connected, fail. Beam-column joints are susceptible to failure earlier than the adjacent members due to the destruction of joint zone. This failure is mainly for the external joints. Therefore, ductility and energy absorption capacity of the beam-column joints are of paramount importance in the seismic resistance of structures (Murthy et al., 2000). Further, reinforcing bars have to meet the requirements of strength and ductility under the repeated reversed deformations. Also, while designing the joint core, it is necessary to verify the shear resistance and anchorage conditions of the reinforcement passing through the joint region.

As per the Indian code of practice for plain and reinforced concrete (BIS, 2000), joints are not specially designed, with the attention being restricted to the provision of sufficient anchorage for the beam longitudinal reinforcement. This may be acceptable when the frame is not subjected to earthquake loads. The poor design practice of beam-column joints is compounded by the high demand imposed by the adjoining flexural members (i.e., beams and columns) in the event of mobilization of their inelastic capacities to dissipate the seismic energy. An unsafe design and detailing within the joint region jeopardizes the entire structure, even if other structural members conform to the design requirements.

Experimental results on the performance of beam-column sub-assemblages of modern structures indicate that current design procedures could sometimes lead to excessive damage of the joint regions

(Tsonos, 2007). Several researchers have studied the influence of axial load on the behaviour of joints under cyclic lateral loading. Uzumeri (1974) tested exterior beam-column sub-assemblages under high constant axial compressive forces and concluded that large axial compressive forces applied to the concrete struts are detrimental to the joints. Bonacci and Pantazopoulou (1993) conducted a parametric investigation of interior joint mechanics based on the variables such as axial load, amount of transverse reinforcement, concrete strength, presence of transverse beams, and bond demand on strength. Agbabian et al. (1993) tested three interior beam-column sub-assemblages with 10%, 5%, and 0% axial load capacities. These test results have indicated that the overall displacement response of sub-assemblages decreases by 22% for a decrease in axial load from 10% to 5% of the squash load. From the above studies, it can be seen that the effect of axial load on the behaviour of joints needs to be verified.

IS 13920 (BIS, 1993) covers the requirements of design and ductile detailing of the reinforced concrete structures subjected to seismic forces. In the proposed revision of IS 13920, guidelines on beam-column joints are included (Jain and Murty, 2005b). The basic requirement of design is that the columns above and below a joint should have sufficient flexural strength when the adjoining beams develop flexural overstrengths at their plastic hinges. This column-to-beam flexural strength ratio is an important parameter to ensure that possible hinging occurs in the beams rather than in the columns or in the joint region. A joint should also have adequate shear strength to avoid the shear failure.

The role of transverse reinforcement and mechanism of shear transfer in a joint for seismic resistance are matters of much debate (Hwang et al., 2005). IS 13920 (BIS, 1993) assumes the role of hoops as to confine the joint core. The real function of hoops may be both to confine the joint core and to carry shear as tension in a tie and hence to constrain the width of cracks. The special confining reinforcement serves three purposes. First, it provides shear resistance to the member. Second, it confines the concrete core and thereby increases the ultimate strain of concrete, which gives greater ductility to the concrete cross-section and enables it to undergo large deformations. Last, it provides lateral restraint against buckling to the compression reinforcement. The experimental studies reveal that the usage of rectangular spiral reinforcement significantly improves the seismic capacity of external beam-column connections (Karayannis et al., 2005).

SCOPE OF THE STUDY

The present work aims mainly at carrying out an experimental investigation to compare the behavior of exterior joints with transverse reinforcement detailed as per IS 456 (BIS, 2000), with additional U-bars as per SP 34 (BIS, 1987b), and IS 13920 (BIS, 1993). The amendments proposed for earthquake analysis and design (Jain and Murty, 2005a, 2005b) are incorporated for arriving at the geometry and reinforcement detailing of all test specimens. The detailing of transverse reinforcement at the joint is chosen as the major variable parameter. The effect of axial load on the behavior of joint is also considered in this study.

ANALYSIS AND DESIGN OF BEAM-COLUMN JOINT

A six-storeyed RC building in the zone III and on the medium soil was analyzed, and the shear forces, bending moments, and axial forces around the exterior beam-column joint due to the induced earthquake loading were calculated. The joint marked “A” in Figure 1 was considered for the design. The columns were 3 m long with 450×300 mm cross-section, and beams were with 300×450 mm cross section. A live load of 3 kN/m^2 and floor finish of 1 kN/m^2 was taken for the analysis. The thicknesses of peripheral and internal walls were taken as 250 mm and 150 mm, respectively. The M30 grade concrete and Fe 415 grade steel were used for the design. The plane frames constituting the joint region were analyzed. The design was carried out based on the proposed amendments (Ingle and Jain, 2005) to IS 1893 (BIS, 2002) and IS 13920 (BIS, 1993). The detailing of transverse reinforcement in the beams, column, and exterior joint were done by considering the detailing criteria of IS 456 (BIS, 2000) and including additional U bars as per SP 34 (BIS, 1987b) for one case, and by incorporating the ductile detailing as per IS 13920 for the second case.

Plane frames were analyzed, and force resultants for various load cases such as dead load, live load, and earthquake load were estimated in the beam AB of the short frame. The design moment and shear force from the critical load combinations for the beam AB were 160.05 kN-m and 112.8 kN, respectively.

The longitudinal reinforcement details of transverse beam and longitudinal beams near the exterior joint are shown in Figures 2(a) and 2(b). The spacing of stirrups on the beam AB near joint was calculated as per IS 456 (BIS, 2000) and as per IS 13920 (BIS, 1993). Two-legged stirrups of 8 mm diameter were provided at a spacing of 100 mm centre to centre near the joint and at 150 mm centre to centre near the mid-span.

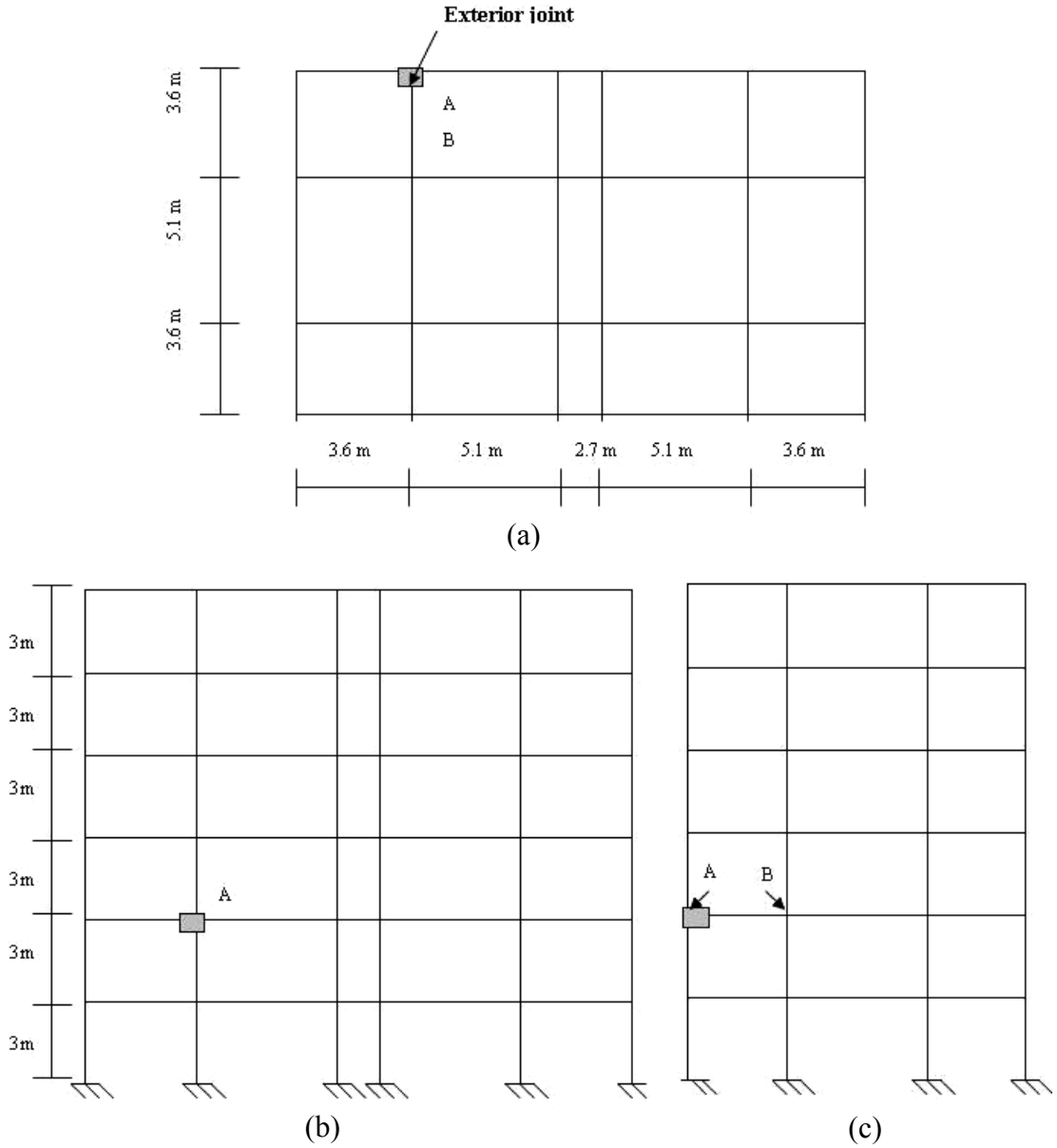

Fig. 1 Details of the building: (a) plan of the building, (b) elevation of the longitudinal frame with the joint A, (c) elevation of the transverse frame with the joints A and B

The exterior column was designed for an axial load of 953 kN and a moment of 86.3 kN-m, which were the critical values obtained from the thirteen different load combinations. Eight 20-mm diameter bars were provided, with the bars distributed equally on all faces of the column. The joint was designed for the strong-column weak-beam condition, for the earthquake ground motion in the X- and Y-directions, as per the draft revision of IS 13920 (BIS, 1993). Special confining reinforcements were provided in the joint region for the detailing as per IS 13920. In the detailing as per the Indian concrete code of practice IS 456 (BIS, 2000), joints were not provided with stirrups, but U-bars were provided for confining the joint core as described by SP 34 (BIS, 1987b).

1. Design of Exterior Joint

The joint shear strength and strong-column weak-beam condition for the earthquake ground motion in the X- and Y-directions were checked as per the draft revision of IS 13920 (BIS, 1993) and were found to be satisfactory.

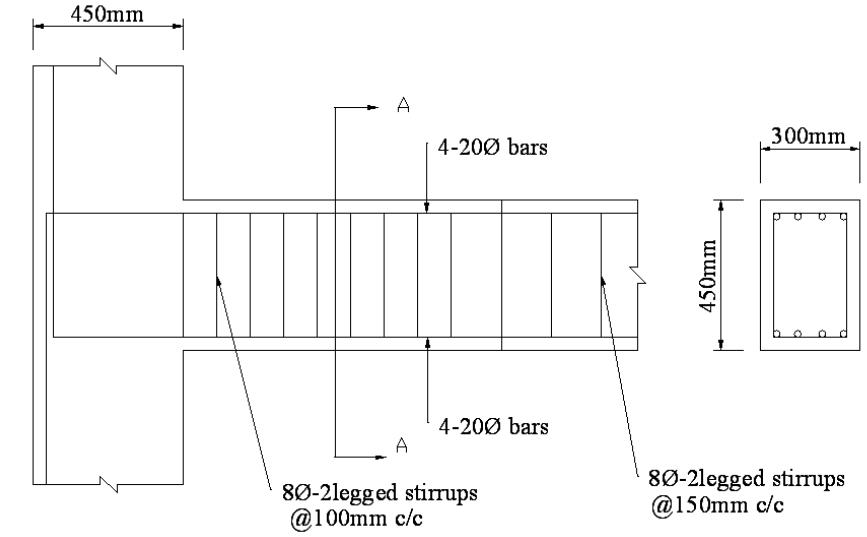

(a)

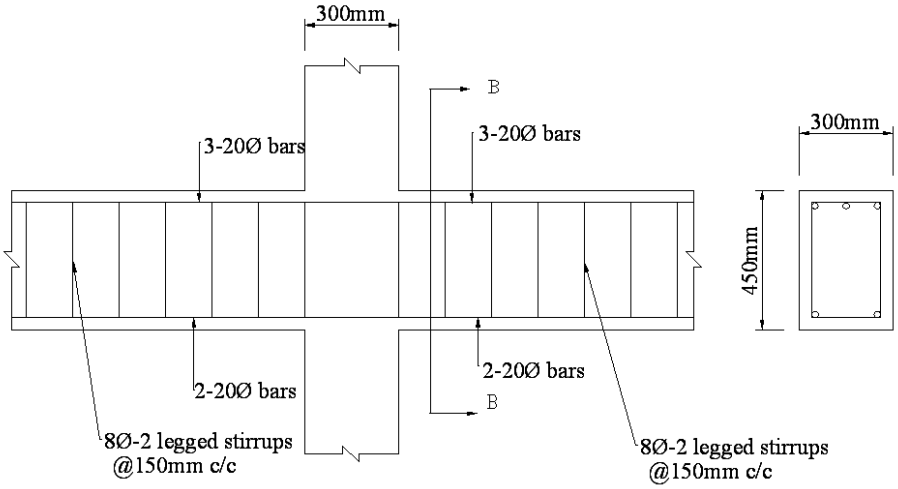

(b)

Fig. 2 (a) Reinforcement details of the transverse beam near the joint A; (b) Reinforcement details of the longitudinal beams near the joint A

Since equal reinforcements were provided at the top and bottom of the transverse beam, V_{col}, the column shear for sway to right or to left during the earthquake loading in the Y-direction, was obtained as 74.50 kN. The force T_1 developed in the top reinforcement of beam was 651.55 kN. Thus, the joint shear force V_{joint} is obtained from Equation (1) as 577.04 kN:

$$V_{joint} = T_1 - V_{col} \tag{1}$$

For the earthquake loading in the X-direction, the column shear for sway to right or to left, V_{col} was obtained as 98.50 kN. The force T_1 developed in the top reinforcement of the right longitudinal beam was 488.66 kN. The force T_2 developed in the bottom reinforcement of the left longitudinal beam was 325.78 kN. Thus, the joint shear force V_{joint} is obtained from Equation (2) as 715.94 kN:

$$V_{\text{joint}} = T_1 + C_2 - V_{\text{col}} \tag{2}$$

where C_2 is the compressive force in the left beam, which is equal to the tensile force T_2 developed in the left beam. The effective width b_j of the joint as per the draft revision of IS 13920 (BIS, 1993) is lesser of (i) $b_j = b_b + 0.5h_c$ and (ii) $b_j = b_c$, where b_b denotes the width of the beam, h_c the depth of the column in the considered direction of shear, and b_c the width of the column.

The effective shear area A_{ej} of the joint is equal to $b_j h_j$, where h_j is the depth of the joint which can be taken as the depth of the column. The shear strength of the joint, $A_{ej}\sqrt{f_{ck}}$, was obtained as 739.43 kN, which is higher than the joint shear force for the earthquake loading in the Y-direction and in the X-direction. Hence, the joint has adequate shear strength in both directions as per the proposed revision. The column-to-beam flexural strength ratios for the earthquake loading in the Y-direction and in the X-direction of the exterior-joint prototype were obtained as 1.84 and 1.39, respectively. Hence, the requirement of strong-column weak-beam condition was satisfied for the earthquake loading in both Y- and X-directions.

Thus, all the joint sub-assemblages considered for the experimental study were checked for shear strength and the strong-column weak-beam theory. The only difference was in the arrangements of transverse reinforcement. Special confining reinforcement was continued in the joint region with detailing as per IS 13920 (BIS, 1993). In the Indian concrete code of practice, IS 456 (BIS, 2000), joints are not provided with stirrups, but U-bars are provided for confining the joint core as in SP 34 (BIS, 1987b).

EXPERIMENTAL PROGRAM

The prototype of the exterior beam-column joint was scaled down to its one-third size. The dimensions and reinforcement details of the test assemblages are shown in Figures 3 and 4 and in Table 1. The specimens were classified into two groups, with two specimens in each group. The specimens in Group 1 were cast with reinforcement detailed as per IS 456 (BIS, 2000). The specimens in Group 2 were detailed as per IS 13920 (BIS, 1993). All the four specimens were tested under constant axial load with cyclic load at the end of the beam. One of the specimens from each group was subjected to an axial load of 3% column axial load capacity and the other specimen was subjected to an axial load of 10% column axial load capacity. The value of axial load on the second specimen was arrived at from the axial force on the upper column of the assemblage at the critical load combination selected for design.

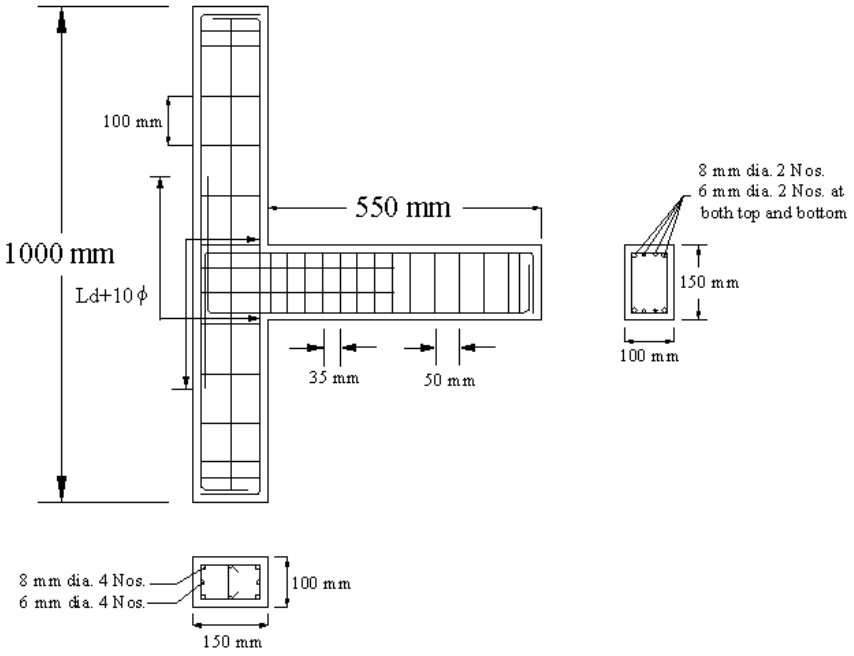

Fig. 3 Reinforcement details of the beam-column joint specimen as per IS 456 (BIS, 2000)

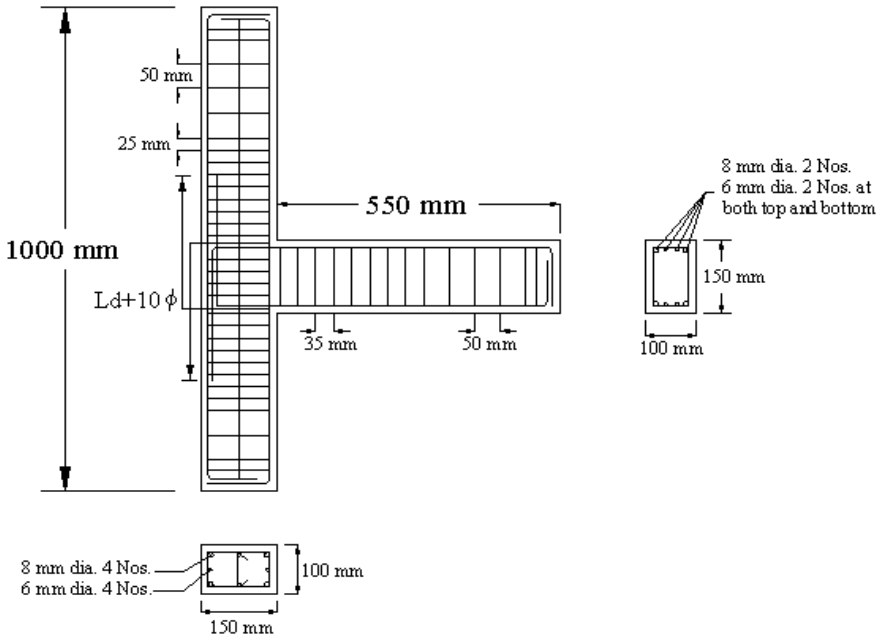

Fig. 4 Reinforcement details of the beam-column joint specimen as per IS 13920 (BIS, 1993)

Table 1: Reinforcement Details of Test Specimens

Specimen Designation	Column Reinforcement		Beam Reinforcement		Joint Reinforcement	Remarks
	Longitudinal	Transverse	Longitudinal	Transverse	Transverse	
A1-456 and A2-456	Four 8-mm diameter and four 6-mm diameter	3-mm diameter at 100 mm centre to centre	Two 8-mm diameter and two 6-mm diameter (at the top and bottom)	3-mm diameter at 35 mm centre to centre for a distance of 270 mm from the joint and 50 mm center to center for the remaining length	Two 3-mm diameter U bars, with development length in tension extended to the beam	No stirrups at the joint, but additional U bars (with hairclip type bend) used for the confinement as per SP 34 (BIS, 1987b)
A1-13920 and A2-13920	Four 8-mm diameter and four 6-mm diameter	3-mm diameter at 25 mm centre to centre for a distance of 230 mm at either side of the joint and 50 mm centre to centre for the remaining portion	Two 8-mm diameter and two 6-mm diameter (at the top and bottom)	3-mm diameter at 35 mm centre to centre for a distance of 270 mm from the joint and 50 mm center to center for the remaining length	3-mm diameter at 25 mm center to centre	Confining reinforcement at the joint as per IS 13920 (BIS, 1993)

1. Casting of Specimens

The specimens were cast by using the 53 grade ordinary Portland cement conforming to IS 12269 (BIS, 1987a). Medium river sand passing through 4.75 mm IS sieve and having a fineness modulus of 2.77 was used as the fine aggregate. Crushed granite stone of maximum size not exceeding 8 mm and having a fineness modulus of 3.58 was used as the coarse aggregate. The mix proportion was 1:0.87:1.32 by weight and the water-cement ratio was kept as 0.48. The 28-day average compressive strength from the 150-mm cube test was 44.22 N/mm^2. The yield stress of reinforcement was 432 N/mm^2. All the specimens were cast in the horizontal position inside a steel mould on the same day. Those were demoulded after 24 hours and were then cured under the wet gunny bags for 28 days.

2. Experimental Setup

The joint assemblages were subjected to the axial load and reverse cyclic loading. The specimens were tested in an upright position and the reverse cyclic loading was applied statically at the end of the beam. One end of the column was given an external hinge support that was fastened to the strong reaction floor, and the other end was laterally restrained by a roller support. A schematic drawing of the setup is shown in Figure 5. The experimental setup at the laboratory is shown in Figure 6.

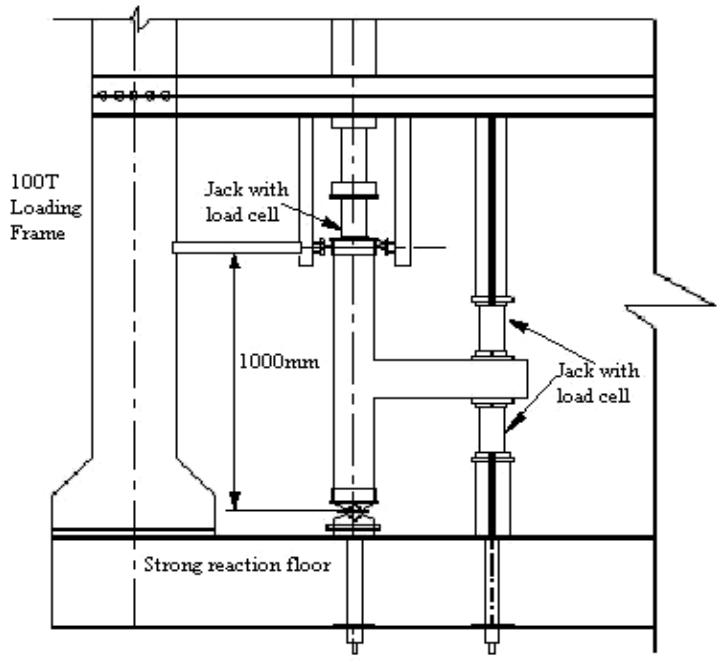

Fig. 5 Schematic diagram of the test set-up

Past theoretical and experimental studies on the influence of the simultaneous changing of the axial load in the column and lateral displacement in the external beam-column joints indicate that significant deterioration is caused in the joint shear strength by the axial load change and P-Δ effect (Tsonos, 2004). It is not the objective of this study to investigate the effect of varying axial load on the response of the sub-assemblages. The influence of the column axial load on the shear capacity of the joints is considered favorable, since the developed principal stresses in the joint are reduced due to the application of compressive axial load, whereas those reach maximum values when the column axial load is null or is neglected (Chalioris et al., 2008). In the present study, the application of the axial load was controlled in order to maintain a constant value during the entire testing procedure.

A constant column axial load was applied by means of a 392.4 kN (40 t) hydraulic jack mounted vertically to the 981 kN (100 t) loading frame to simulate the gravity load on the column. The axial load was 15.92 kN (1.62 t) for the first-series specimens and 53.06 kN (5.41 t) for the second-series specimens. The cyclic loading was applied by two 196.2 kN (20 t) hydraulic jacks, one fixed to the loading frame at the top and another to the strong reaction floor. The reverse cyclic load was applied at 50 mm from the free end of the beam portion of the assemblage. The test was load-controlled and the specimen was subjected to an increasing cyclic load up to its failure.

Fig. 6 Test setup in the laboratory

In order to utilize the results obtained from a quasi-static cyclic loading test on structural elements for a general performance evaluation there is a need to establish a loading history that captures the critical issues of the element capacity as well as of the seismic demands. The basic seismic capacity parameters for a structural element are strength, stiffness, inelastic deformation capacity (i.e., ductility), and cumulative damage capacity parameters such as energy dissipation capacity. All these parameters are expected to deteriorate as the number of damaging cycles and the amplitude of cycles increase (Karayannis and Sirkelis, 2008; Chalioris et al., 2008). In order to draw conclusions for the ultimate limit state and to evaluate the performance under arbitrary seismic excitations, a cyclic loading sequence with constantly increasing load and large inelastic excursions was chosen. It may also be emphasised that there is a significant dependence of the demand parameters on the natural period of the structure, of which the structural element is a member. For generic test specimens, there exists a need to obtain these parameters for short-period structures, with the understanding that their values may be very conservative for the long-period structures.

The load increment chosen was 1.962 kN (200 kg). The loading protocol consists only of one cycle, and repeat cycles were not employed. The specimen was first loaded up to 1.962 kN and unloaded and was then reloaded in the reverse direction up to 1.962 kN. The subsequent cycles were also loaded in a similar way. Figure 7 shows the loading sequence of the test assemblages. To record the loads precisely, load cells with the least count of 0.0981 kN were used. The specimens were instrumented with a linear variable differential transformer (LVDT) with the least count of 0.1 mm to measure the deflection at the loading point. A clinometer was fixed on top of the beam element of the specimen to measure rotation near the interface during the loading.

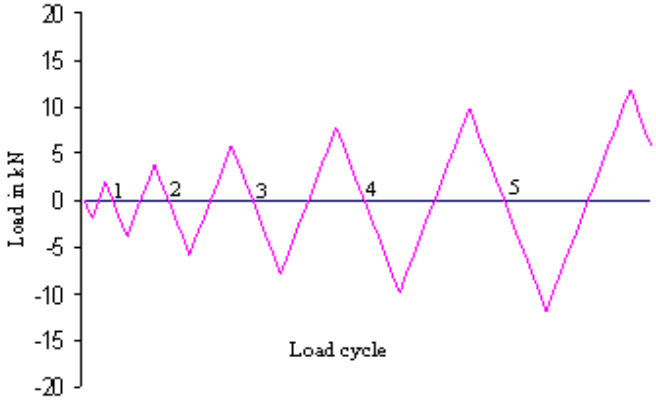

Fig. 7 Sequence of cyclic loading

DISCUSSION OF TEST RESULTS

The test results are presented in the form of load-deformation hysteretic curves, envelope curves for load-displacement, energy dissipation curves, stiffness degradation curves, and damage-index and moment-rotation envelopes. The observations made during the test are briefly described in the following sections.

1. Cracking Pattern and Failure Mode

In all specimens in the first series (with the axial load of 15.92 kN) the initial diagonal hairline crack on the joint occurred at the second loading cycle, when the load reached 3.924 kN in both positive and negative cycles of loading. However, for the second series (with the axial load of 53.06 kN), the first crack appeared only in the third cycle for a load of 5.886 kN in all specimens. The yield and ultimate loads for the test specimens are shown in Table 2. The specimens in the two series performed in the same manner for their ultimate strengths. However, the axial load improved the cyclic load carrying capacity of the joint. The cracking patterns of the test specimens in the first and second series are shown in Figures 8 and 9, respectively. In almost all specimens, tensile cracks were formed at the interface between the column and beam. The specimens failed due to the advancement of crack width at the interface between the beam and the column. There was a clear vertical cleavage formed at the junction of all specimens. In addition to that, for the first-series specimens, there were some hairline cracks in the joint region. The second-series specimens were tested under the increased axial load, and it may be observed that the performance improved due to the increase in axial load.

Table 2: Experimental Yield and Ultimate Loads of Specimens

Designation of Specimen	Experimental Yield Load (kN)			Experimental Ultimate Load (kN)		
	Downward Direction	Upward Direction	Average (P_{ye})	Downward Direction	Upward Direction	Average (P_{ue})
A1-456	13.73	11.77	12.75	15.69	14.71	15.2
A1-13920	11.77	11.77	11.77	16.18	15.69	15.93
A2-456	15.7	13.7	14.7	18.64	18.64	18.64
A2-13920	15.7	15.7	15.7	17.66	19.62	18.64

Similar to the first series, the specimens in the second series failed due to the vertical cleavage at the beam-column joint interface. Thus, with beam failure having preceded the joint failure, it can be seen that all the specimens have satisfied the strong-column weak-beam theory.

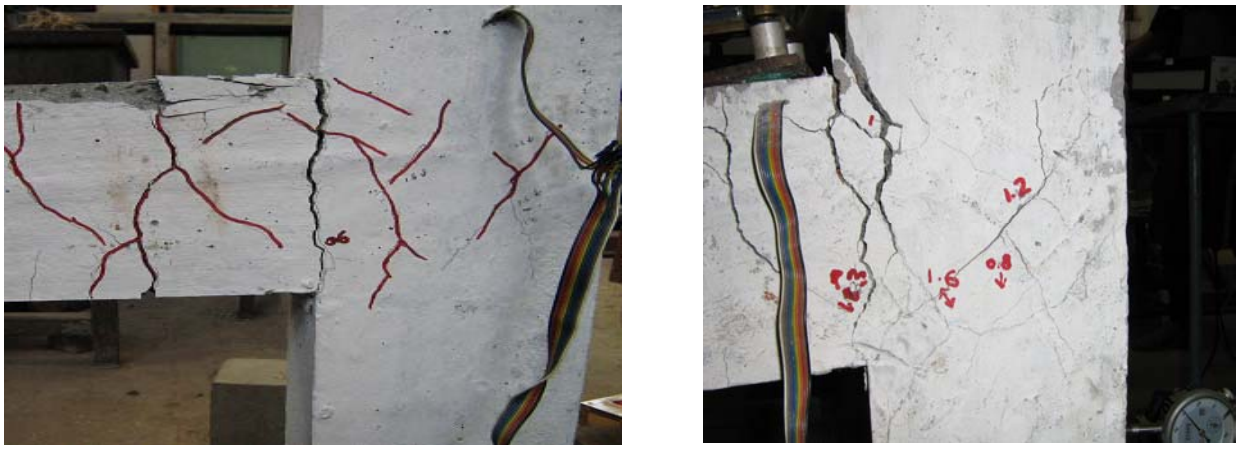

(a) (b)

Fig. 8 Crack patterns in the specimens in the first series for (a) Specimen A1-456 and (b) Specimen A1-13920

(a) (b)

Fig. 9 Crack patterns in the specimens in the second series for (a) Specimen A2-456 and (b) Specimen A2-13920

2. Hysteretic Loops

The force-displacement hysteretic loops for the specimens are shown in Figures 10 to 13. It is seen from Table 2 that the ultimate load carrying capacity is increased with an increase in axial load. A relative comparison of the overall force-deformation behavior of all specimens in the first and second series is shown in Figure 14.

3. Energy Dissipation

The area enclosed by the hysteretic loop in a given cycle represents the energy dissipated by the specimen during that cycle. Figure 15 shows the cumulative energy dissipated versus cumulative displacement curve of all specimens. The highest energy dissipated (i.e., 995.5436 kN-mm) was for Specimen A1-13920. It may be observed that an increase in the axial load reduces the energy dissipation capacity of specimens. However, the specimens with higher axial loads are found to have sustained greater number of cycles of the seismic type loads than the specimens with lesser axial loads.

4. Member Flexural Strength

The section capacities are designed to have the ratio $\sum M_c / \sum M_b$ of 2.3 for all specimens to ensure that the beams fail before the column. The design and experimental member flexural capacities of the specimens are shown in Table 3. The experimental values of the member capacities show that the specimens have satisfied the strong-column weak-beam concept.

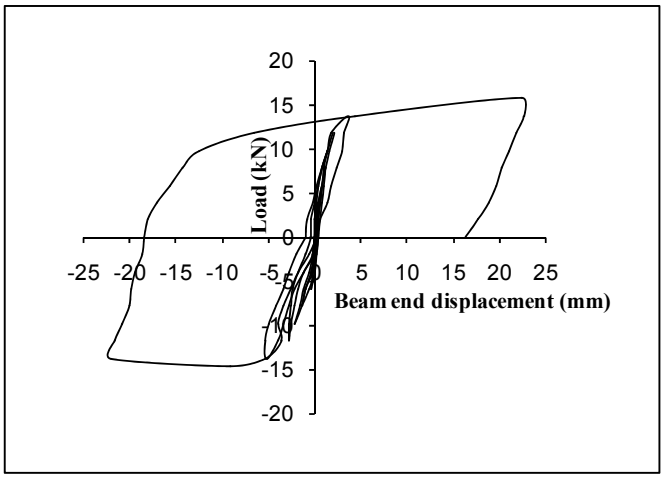

Fig. 10 Load versus displacement curve of Specimen A1-456

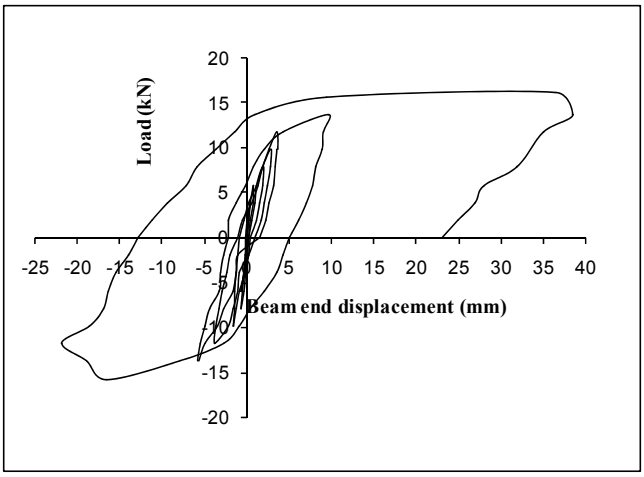

Fig. 11 Load versus displacement curve of Specimen A1-13920

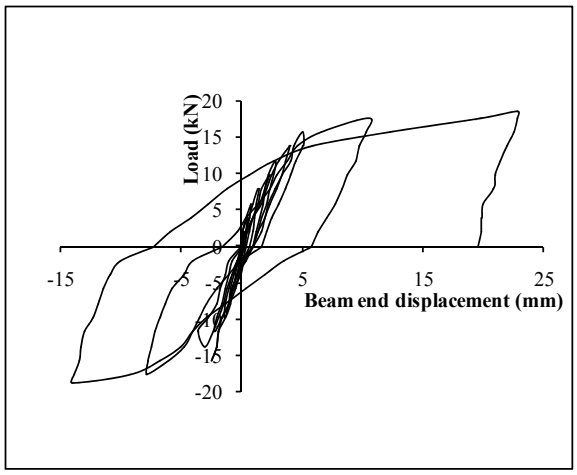

Fig. 12 Load versus displacement curve of Specimen A2-456

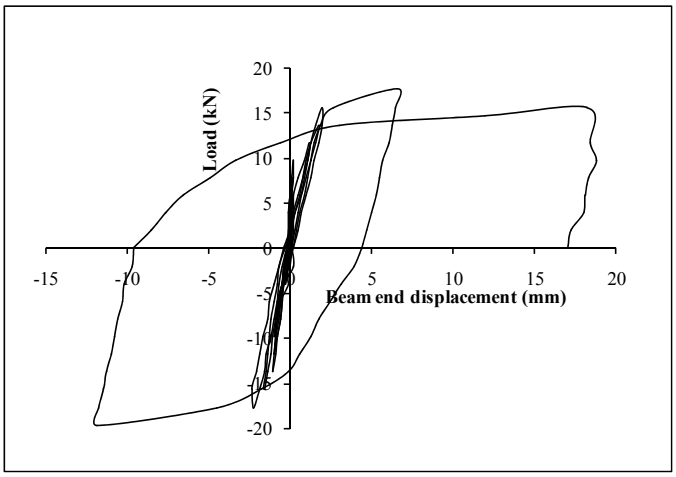

Fig. 13 Load versus displacement curve of Specimen A2-13920

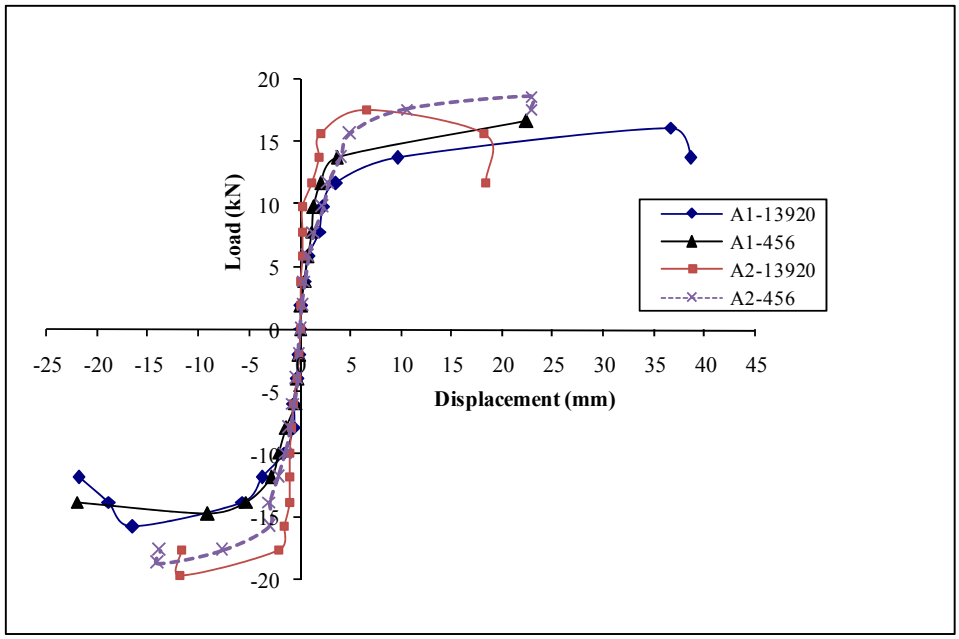

Fig. 14 Load-displacement envelops of the four specimens

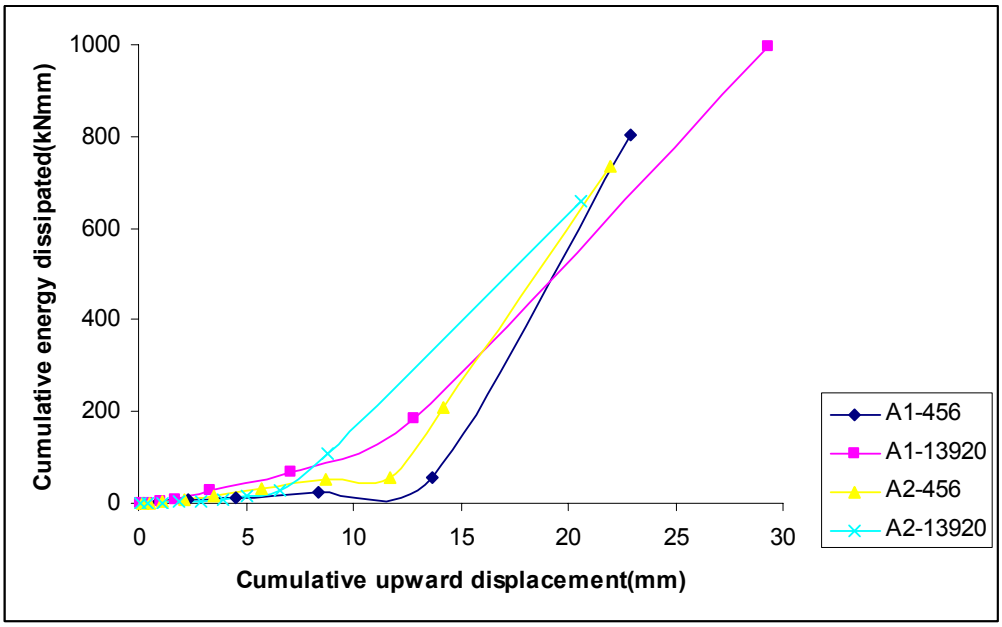

Fig. 15 Cumulative energy dissipation curves of the four specimens

Table 3: Member Flexural Strengths of Test Specimens

Designation of Specimen	Beam Moment Strength (kN-m)			Column Moment Strength (kN-m)			$\frac{\sum M_c}{\sum M_b}$	
	Design	Experimental		Design	Experimental			
		Yield Strength	Over-strength		Yield Strength	Over-strength	Yield Strength	Over-strength
A1-456	5.91	6.865	7.36	5.47	7.90	8.46	2.3	2.3
A1-13920	5.91	6.865	7.85	5.47	7.90	9.02	2.3	2.3
A2-456	5.91	7.85	9.32	5.47	9.03	10.72	2.3	2.3
A2-13920	5.91	7.85	9.81	5.47	9.03	11.28	2.3	2.3

5. Joint Stresses

The horizontal shear stress in the exterior joint sub-assemblage can be expressed as (Murty et al., 2003)

$$\tau_{jh} = \frac{P}{A^h_{\text{core}}}\left(\frac{L_b}{d_b} - \frac{L_b + 0.5D_c}{L_c}\right) \tag{3}$$

where P denotes the imposed cyclic load at the end of the beam, L_b the length of the beam, L_c the length of the column, D_c the total depth of the beam, d_b the effective depth of the beam, and A^h_{core} the horizontal cross-sectional area of the joint core resisting the horizontal shear force.

It is necessary to limit the magnitude of the horizontal joint shear stress to protect the joint against diagonal crushing. The ACI-318 standard (ACI, 2002) limits the horizontal joint shear stress (in MPa) as $k\sqrt{f_c'}$, where f_c' is the cylinder compressive strength in MPa. The factor k depends on the confinement provided by the members framing into the joint; k is taken as 1.67, 1.25, and 1.0 for the interior, exterior, and corner joints, respectively.

The ultimate values of the horizontal shear stress induced in the joints are found to be almost equal to or little higher than the ACI-recommended values (ACI, 2002). It may be seen from Table 4 that the shear-resisting capacity is more for the specimens detailed according to IS 13920 (BIS, 1993) than for the specimens detailed according to IS 456 (BIS, 2000) and provided with additional U-bars. Further, an increase in the axial load improves the shear capacity of joints. From the values of $\tau_{jh}/\tau_{\text{ACI}}$, it may be seen that the specimens with higher axial loads exhibit higher shear capacity. Even at lower axial load levels, the specimens have shear capacity close to the ACI-prescribed limiting value (ACI, 2002). Hence, the design of longitudinal reinforcement and geometry of the section as per the proposed revisions (Jain and Murty, 2005a, 2005b) appear to be adequate.

Table 4: Comparison of Ultimate Joint Shear Stress with the ACI Code-Prescribed Limiting Values

Designation of Specimen	H_u (kN)	H_{ucalc} (kN)	$\frac{H_u}{H_{ucalc}}$	τ_{jh} (MPa)	$\frac{\tau_{jh}}{\tau_{\text{ACI}}}$
A1-456	14.71	14.1	1.04	5.48	0.92
A1-13920	15.69	14.1	1.11	5.84	0.98
A2-456	18.64	14.1	1.32	6.94	1.16
A2-13920	19.62	14.1	1.39	7.31	1.23
With f_c' = 35.376 MPa, the maximum permissible shear stress τ_{ACI} is equal to 5.95 MPa.					

The principal tensile stress (i.e., diagonal tensile stress) developed in the beam-column joint region is calculated as

$$\sigma_t = \frac{\sigma_p}{2} + \sqrt{\frac{\sigma_p^2}{4} + \tau_{jh}^2} \tag{4}$$

where $\sigma_p = (N_c + P)/b_c h_c$ is the axial compressive stress in the joint area; τ_{jh} is the joint horizontal shear stress; N_c is the axial compressive load in the column; and P is the imposed cyclic load at the end of the beam.

On computation of τ_{jh} using Equation (3), Figure 16 shows the variation of principal stress in the joint with storey drift. From the figure it is deduced that the principal stress developed in the specimens detailed as per IS 13920 (BIS, 1993), i.e., A1-13920 and A2-13920, is higher than that for the corresponding specimens detailed as per IS 456 (BIS, 2000), i.e., A1-456 and A2-456.

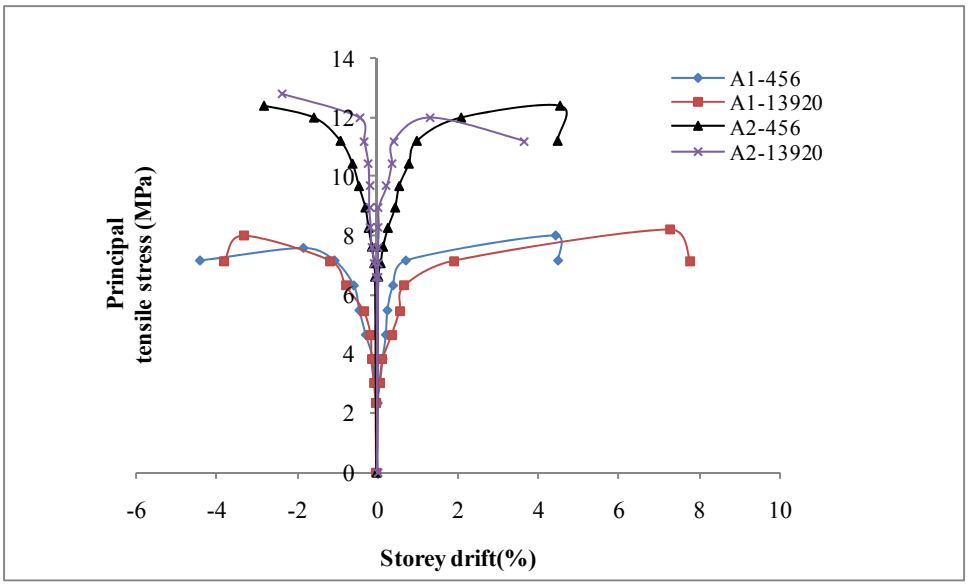

Fig. 16 Principal tensile stresses of the tested specimens

6. Damage Index

To assess the effectiveness of joints, the damage index model by Park and Ang (1985) is employed in this study. This model is based on the concept that seismic structural damage can be expressed as a linear combination of the damage caused by excessive deformation and the damage accumulated due to the repeated cyclic loading effect (Sreekala et al., 2007). In terms of damage index this model may be described as

$$D = \frac{\delta_M}{\delta_u} + \frac{\beta}{Q_y \delta_u} \int \mathrm{d}E \tag{5}$$

where δ_M is the maximum deformation under the earthquake ground motion; δ_u is the ultimate deformation under the monotonic loading; Q_y is the calculated yield strength; $\mathrm{d}E$ is the incremental absorbed hysteretic energy; and β is a non-negative parameter representing the effect of cyclic loading on structural damage. Value of the parameter β is determined in such a way that it represents the nature of damage in the examined specimen as closely as possible.

The confinement ratios for Specimens A1-456 and A2-456 are calculated by considering the additional U-bars in the joint region. The values of damage index by Park and Ang (1985) are presented in Figure 17. From the results it is evident that Specimens A1-13920 and A2-13920 have undergone a lower damage than Specimens A1-456 and A2-456, respectively.

7. Stiffness

The stiffness of the beam-column joint is approximated as slope of the peak-to-peak line in each loading cycle (Park and Paulay, 1975; Tsonos, 2000; El-Amoury and Ghobarah, 2002). The variation of stiffness in each cycle corresponding to the maximum displacement in that cycle is calculated and is shown in Figure 18. It may be observed that the stiffness was highest for Specimen A2-13920, and for this specimen, the major reduction in stiffness occurred only after the sixth cycle of loading. Specimen A1-13920 had greater stiffness than Specimens A1-456 and A2-456. This specimen also reached a higher ductility level than the other specimens. While considering the influence of axial load, it may be seen from Figure 18 that the presence of axial load stiffened the joint.

8. Moment-Rotation Relation

The envelope curve for the moment in beam near the interface of the sub-assemblage and the rotation of the beam element during the downward loading in each cycle are shown in Figure 19. It may be

observed that the rotation was higher for the first-series specimens than for the second-series specimens. Further, Specimens A1-13920 and A2-13920 have exhibited good rotational ductility.

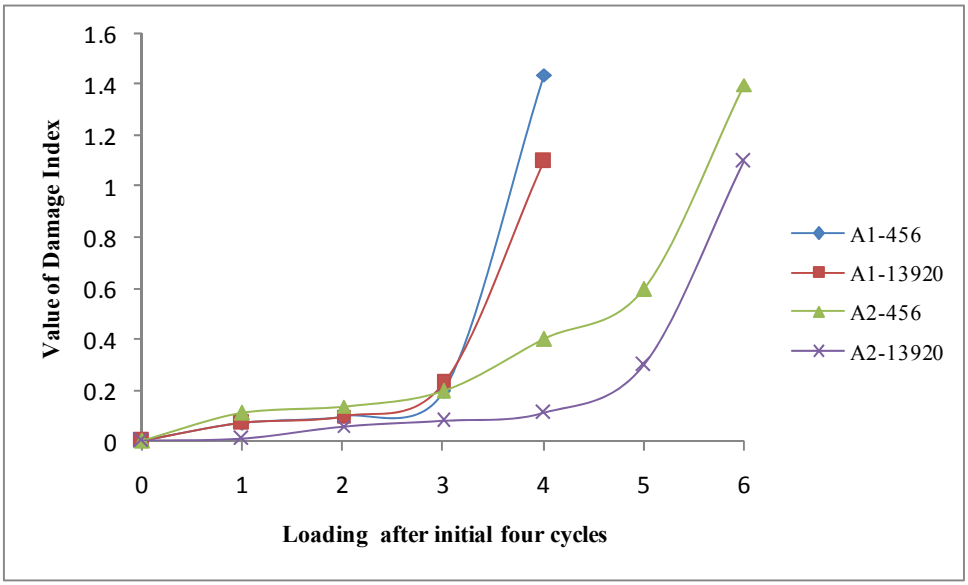

Fig. 17 Comparison of the Park and Ang damage indices of the tested specimens

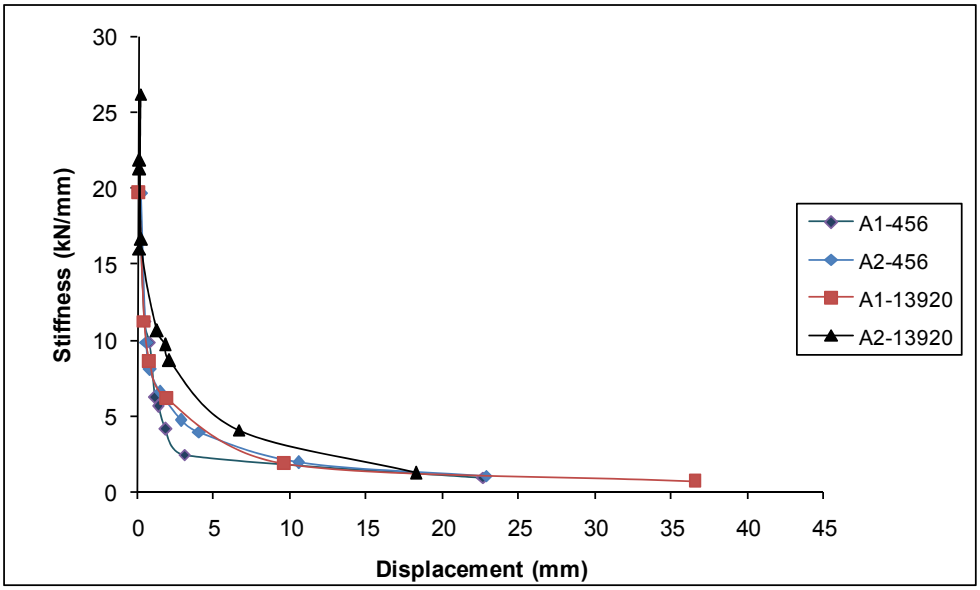

Fig. 18 Stiffness degradation of the specimens

CONCLUSIONS

The purpose of this investigation was to evaluate the performance of the exterior beam-column joints designed and detailed as per the proposed amendments of IS 1893 (BIS, 2000) and IS 13920 (BIS, 1993) for the earthquake-resistant design. All the specimens were designed for adequate shear strength in the joint and to satisfy the strong-column weak-beam theory. One set of specimens was made with the special confining reinforcement as per the provisions of IS 13920. The effect of special confining reinforcement on the behaviour of joint has been studied by comparing the test results of the companion specimens detailed without the special confining reinforcement but with the transverse reinforcement as required by IS 456 (BIS, 2000) and SP 34 (BIS, 1987b). Following conclusions have been drawn from this study:

1. All the specimens failed due to the development of tensile cracks at the interface between beam and column, and this has ensured that the strong-column weak-beam conditions were satisfied.

2. The joint region was free from cracks except for some hairline cracks, and therefore the joints had adequate shear-resisting capacity.
3. An increase in the column axial load improves the load carrying capacity and stiffens the joints. However, this reduces the energy absorption capacity and ductility of the joint.
4. The specimens having special confining reinforcement as per IS 13920 (BIS, 1993) had an improved energy absorption capacity than the specimens with lateral reinforcement detailing as per IS 456 (BIS, 2000) and SP 34 (BIS, 1987b).

In the present study, for all the specimens the cracks were concentrated at the beam-column interface and not in the beam region. Hence, there is a necessity to develop a detailing pattern of the sub-assemblages in order to shift the plastic hinge towards the beam region.

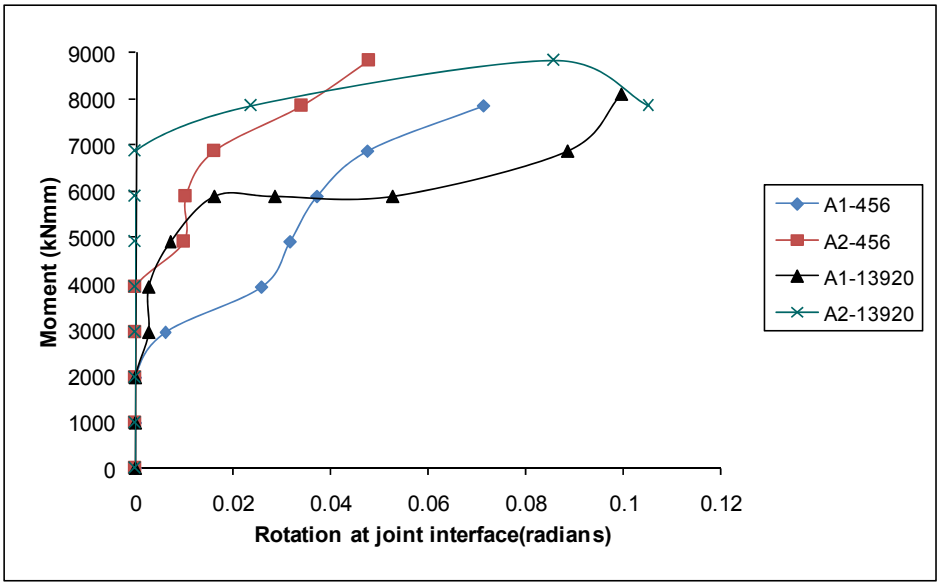

Fig. 19 Moment-rotation relation of the beam element of specimens

NOTATIONS

A_{core}^{h} = horizontal cross-sectional area of the joint core resisting horizontal shear force

A_{ej} = effective shear area of joint

b_b = width of beam

b_c = width of column

b_j = effective width of joint

C_2 = compressive force in the left beam

d_b = effective depth of beam

D_c = total depth of beam

$f_c^{'}$ = cylinder compressive strength of concrete

h_c = depth of column in the considered direction of shear

h_j = depth of joint which can be taken as depth of column

k = factor which depends on confinement provided by the members framing into joint

L_b = length of beam

L_c = length of column

N_c = column axial compressive load

P = imposed cyclic load at the end of beam

Q_y = calculated yield strength

T_1 = force developed in the top reinforcement of beam

T_2 = force developed in the bottom reinforcement of beam

V_{joint} = joint shear force

V_{col} = column shear for sway to right or left during the earthquake loading in Y- or X-direction

β = non-negative parameter representing the effect of cyclic loading on structural damage

σ_p = axial compressive stress in the joint area

τ_{jh} = joint horizontal shear stress

δ_M = maximum deformation under earthquake ground motion

δ_u = ultimate deformation under monotonic loading

$\mathrm{d}E$ = incremental absorbed hysteretic energy

REFERENCES

1. ACI (2002). "Building Code Requirements for Structural Concrete (ACI 318-02) and Commentary (ACI 318R-02)", ACI Standard, American Concrete Institute, Farmington Hills, U.S.A.
2. Agbabian, M.S., Higazy, E.M., Abdel-Ghaffar, A.M. and Elnashai, A.S. (1994). "Experimental Observations on the Seismic Shear Performance of RC Beam-to-Column Connections Subjected to Varying Axial Column Force", Earthquake Engineering & Structural Dynamics, Vol. 23, No. 8, pp. 859–876.
3. BIS (1987a). "IS 12269: 1987—Indian Standard Specification for 53 Grade Ordinary Portland Cement", Bureau of Indian Standards, New Delhi.
4. BIS (1987b). "SP 34: 1987—Handbook on Concrete Reinforcement and Detailing", Bureau of Indian Standards, New Delhi.
5. BIS (1993). "IS 13920: 1993—Indian Standard Ductile Detailing of Reinforced Concrete Structures Subjected to Seismic Forces—Code of Practice", Bureau of Indian Standards, New Delhi.
6. BIS (2000). "IS 456: 2000—Indian Standard Plain and Reinforced Concrete—Code of Practice (Fourth Revision)", Bureau of Indian Standards, New Delhi.
7. BIS (2002). "IS 1893 (Part 1): 2002—Indian Standard Criteria for Earthquake Resistant Design of Structures, Part 1: General Provisions and Buildings (Fifth Revision)", Bureau of Indian Standards, New Delhi.
8. Bonacci, J. and Pantazopoulou, S. (1993). "Parametric Investigation of Joint Mechanics", ACI Structural Journal, Vol. 90, No. 1, pp. 61–71.
9. Chalioris, C.E., Favvata, M.J. and Karayannis, C.G. (2008). "Reinforced Concrete Beam-Column Joints with Crossed Inclined Bars under Cyclic Deformations", Earthquake Engineering & Structural Dynamics, Vol. 37, No. 6, pp. 881–897.
10. El-Amoury, T. and Ghobarah, A. (2002). "Seismic Rehabilitation of Beam-Column Joint Using GFRP Sheets", Engineering Structures, Vol. 24, No. 11, pp. 1397–1407.
11. Hwang, S.-J., Lee, H.-J., Liao, T.-F., Wang, K.-C. and Tsai, H.-H. (2005). "Role of Hoops on Shear Strength of Reinforced Concrete Beam-Column Joints", ACI Structural Journal, Vol. 102, No. 3, pp. 445–453.

12. Ingle, R.K. and Jain, S.K. (2005). "Explanatory Examples for Ductile Detailing of RC Buildings", Report IITK-GSDMA-EQ22-V3.0, IIT Kanpur, Kanpur.
13. Jain, S.K. and Murty, C.V.R. (2005a). "Proposed Draft Provisions and Commentary on Indian Seismic Code IS 1893 (Part 1)", Report IITK-GSDMA-EQ05-V4.0/IITK-GSDMA-EQ15-V3.0, IIT Kanpur, Kanpur.
14. Jain, S.K. and Murty, C.V.R. (2005b). "Proposed Draft Provisions and Commentary on Ductile Detailing of RC Structures Subjected to Seismic Forces", Report IITK-GSDMA-EQ11-V4.0/IITK-GSDMA-EQ16-V3.0, IIT Kanpur, Kanpur.
15. Karayannis, C.G. and Sirkelis, G.M. (2008). "Strengthening and Rehabilitation of RC Beam-Column Joints Using Carbon-FRP Jacketing and Epoxy Resin Injection", Earthquake Engineering & Structural Dynamics, Vol. 37, No. 5, pp. 769–790.
16. Karayannis, C., Sirkelis, G. and Mavroeidis, P. (2005). "Improvement of Seismic Capacity of External Beam-Column Joints Using Rectangular Spiral Shear Reinforcement", Proceedings of the Fifth World Conference on Earthquake Resistant Engineering Structures (ERES V), Skiathos, Greece, pp. 147–156.
17. Murthy, D.S.R., Gandhi, P., Sreedhar, D.S., Vaidhyanathan, C.V. and Mohanty, O.N. (2000). "Seismic Resistance of Reinforced Concrete Beam-Column Joints with TMT and CRS Bars", ICI Journal, Vol. 1, No. 3, pp. 19–26.
18. Murty, C.V.R., Rai, D.C., Bajpai, K.K. and Jain, S.K. (2003). "Effectiveness of Reinforcement Details in Exterior Reinforced Concrete Beam-Column Joints for Earthquake Resistance", ACI Structural Journal, Vol. 100, No. 2, pp. 149–156.
19. Park, R. and Ang, A.H.S. (1985). "Mechanistic Seismic Damage Model for Reinforced Concrete", Journal of Structural Engineering, ASCE, Vol. 111, No. 4, pp. 722–739.
20. Park, R. and Paulay, T. (1975). "Reinforced Concrete Structures", John Wiley & Sons, Inc., New York, U.S.A.
21. Sreekala, R., Lakshmanan, N., Kumar, K.S. and Gopalakrishnan, N. (2007). "Evaluation of Damage Indices for RC Beams under Cyclic Loading—A Simple Technique", Journal of Structural Engineering, SERC, Vol. 34, No. 1, pp. 40–47.
22. Subramanian, N. and Rao, D.S.P. (2003). "Seismic Design of Joints in RC Structures—A Review", Indian Concrete Journal, Vol. 77, No. 2, pp. 883–892.
23. Tsonos, A.G. (2000). "Effect of Vertical Hoops on the Behaviour of Reinforced Concrete Beam-to-Column Connections", European Earthquake Engineering, Vol. XIV, No. 2, pp. 13–26.
24. Tsonos, A.G. (2004). "Improvement of the Earthquake Resistance of R/C Beam-Column Joints under the Influence of P-Δ Effect and Axial Force Variations Using Inclined Bars", Structural Engineering and Mechanics, Vol. 18, No. 4, pp. 389–410.
25. Tsonos, A.G. (2007). "Cyclic Load Behavior of Reinforced Concrete Beam-Column Subassemblages of Modern Structures", ACI Structural Journal, Vol. 104, No. 4, pp. 468–478.
26. Uzumeri, S.M. (1974). "Strength and Ductility of Cast-in-Place Beam-Column Joints", Proceedings of the Symposium on Reinforced Concrete Structures in Seismic Zones, San Francisco, U.S.A., pp. 293–350.